CAAP Quarterly Report

Date of Report: October 10, 2016
Contract Number: DTPH5615HCAP03
Prepared for: James Prothro, PHMSA-DOT
Project Title: Bayesian Network Inference and Information Fusion for Accurate Pipe Strength and Toughness Estimation
Prepared by: Arizona State University, University of Colorado-Denver, and Michigan State University
Contact Information: Dr. Yongming Liu and Dr. Yiming Deng
For quarterly period ending: October 10, 2016

Business and Activity Section:

ASU Student training activities

- Sonam Dahire works on the material specimen preparation, testing, and data analysis;
- Sonam Dahire and Tishun Peng work on the Bayesian inference with experimental measurements;
- Ankita Kardile works on the numerical and experimental testing for the ABI testing for strength estimation;
- Sonam Dahire and Ankita Kardile write the report.

CU Denver student training activities

(The research team has moved to Michigan State University since Fall 2016)

- Xiaodong Shi works on multi-physics modeling, numerical algorithms development and analysis, as well as fast continuous imaging protocol design and implementation
- Salem Egdaire works on NMMI amplitude and phase imaging development
  Xiaodong Shi and Deepak Kumar works on the experimental testing for data fusion and correlations between electromagnetic measurements and mechanical measurements
- Deepak Kumar works on the compressed sensing assisted fast imaging development
- Xiaodong Shi and Deepak Kumar write the report

(a)Generated Commitments

The system for natural gas pipelines in the United States consists of a network to gather, transport and distribute the product, which consists of 210 systems overall running through the different states. Pipeline infrastructure forms a vital aspect in improving the U.S. economy and standard of living A major portion of the current operational pipelines have been installed in the early 1900's, and therefore lack reliable information on the integrity of the aging pipeline systems which is a critical safety concern. The conventional methods of inspection such as pipeline inspection gauge (PIG) cannot be used to inspect about three-fourth of the present pipeline systems, due to the pipes being too old/ twists/turns etc. which does not allow PIGs to operate in them. In order to maintain the safety and economy standards, accurate estimation of pipe strength and toughness without interrupting the transmission and operations of the pipelines is crucial. Many of the existing techniques focus on single modality measurement for the narrow surface layer measurements and cannot capture decarburization and manufacturing process-induced material inhomogeneity. Also, uncertainties exist in terms of material properties, pipe geometries, manufacturing process, operational conditions, etc., leading to gaps in the accurate strength and toughness determination. Therefore, a novel approach using multimodality diagnosis and information fusion framework has been proposed for probabilistic pipe strength and toughness estimation, which is the objective of the present work. The first part of the project will consist of estimating the basic material properties; microstructure, composition etc. as well as various surface mechanical properties and studying their variation with thickness of the pipeline samples. The second part compromises of advanced testing methods for property estimation with the use of acoustic and electromagnetic sensors. And finally, the information obtained from the two parts would be integrated with the statistical correlations into a multimodal system to obtain a probabilistic strength and toughness with a high degree of accuracy. The typical pipeline grades include A, B, X42, and X46 as distribution pipelines, and X52, X56, X60, X65, X70, X80 etc. for transmission. The latter grades such as X65-X120 have been manufactured through advanced processing methods which imparts a better control on the mechanical properties. However, due to the conventional processing methods for the earlier grades, a large variation in the properties has been observed. These earlier grades still form a vital part of the current service pipelines, hence, a reliable source of information of the aging systems is essential, and therefore form the focus of our study.

Several major tasks are proposed to address the above-mentioned project objectives/goals. Experimental testing, advanced data analysis, numerical simulation, and probabilistic methods are integrated in the proposed tasks. A summary is listed below and detailed work plan will be discussed in the following sections.

Task 1. Experimental testing and data analysis of chemical, metallurgical, and mechanical properties of pipe steel (Arizona State University)

This task focuses on the information obtaining and analysis about the basic pipe steel properties. Both in-house experimental testing and literature data will be used for this

task. First, in situ and ex situ chemical composition analysis will be performed for several representative pipe steel specimens (from online vendors and our industry collaborators). Optical emission spectrography (OES) and energy dispersive spectroscopy (EDS) will be used for in situ and ex situ measurements of chemical composition, respectively. Following this, in situ and ex situ pipe steel microstructure analysis will be performed to obtain the grain structure images using etchingbased optical microscopy and electron back scattered diffraction (EBSD) images, respectively. Imaging analysis will be performed to obtain the statistical information and metrics about the pipe steel microstructure, such as grain size distribution. Next, surface hardness measurements will be performed using portable ultrasound hardness testers and the results will be correlated with pipe strength and toughness. Advanced data analysis using Gaussian Process modeling will be used for surrogate modeling and to quantify the uncertainties for future Bayesian network inference.

Task 2. Experimental testing, data analysis and prototyping for acoustic and microelectromagnetic electromagnetic properties of pipe steel (University of Colorado-Denver)

This task focuses on the information obtaining and analysis about the pipe steel acoustic and micro-electromagnetic properties. First, ex situ low-frequency near-field microwave microscopy analysis will be performed for several representative pipe steel specimens. Obstacles for dislocation movement, such as grain boundaries and void inclusions, will be revealed in terms of measurable electromagnetic properties. Following that, surface and subsurface microstructural image analysis assisted by Multiphysics modeling will be carried out to understand the correlations between steel strength and different possible mechanisms which impede the dislocation movement under load in the micro electromagnetic spectrum. Next, a prototype of integrating magnetostriction and pulsed eddy current-based Barkhausen noise imaging system will be developed to characterize the pipe steel's Bloch wall jumps and the results will be correlated with pipe strength and toughness experimentally with advanced data analysis.

Task 3. Bayesian network for information fusion and probabilistic pipe strength estimation (Arizona State University and University of Colorado-Denver)

This task will focus on the development of a novel Bayesian network for the inference of pipe strength and toughness. First, the network structure and conditional probability estimation will be performed using the multi-modality diagnosis data obtained in Tasks 1&2. Following this, parametric studies with synthetic data using the developed Bayesian network will be performed to investigate the behavior and performance of the information fusion framework. Sensitivity analysis will be performed to identify the important factors in the proposed Bayesian network. Finally, model verification and validation with realistic field/laboratory measurements will be demonstrated. Probabilistic pipe strength estimation and associated risk-based confidence determination will be quantified.

A schematic illustration of the proposed components and their integration is shown in Fig.1. The philosophy behind the proposed methodology is that each modality diagnosis will contain part of the information about the pipe steel strength and a fusion process will, in principle, provide more accurate estimation of the current state of the aging pipes. This schematic illustration also indicates the multidisciplinary collaborative work of the proposed study. Mechanical and material research (ASU), electromagnetic and acoustic study (CU-Denver), and industrial experiences (GTI) are integrated together for the probabilistic pipe strength estimation and future decision making for risk mitigation.

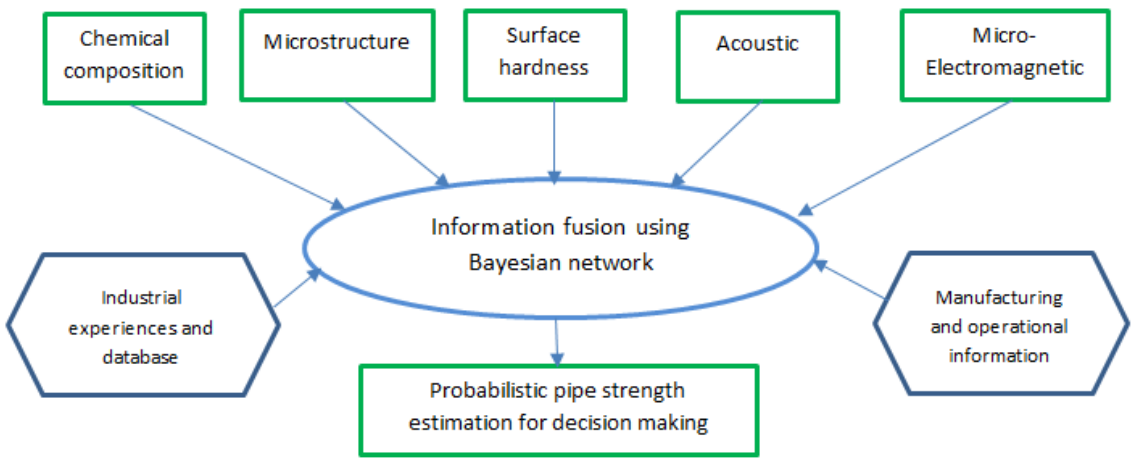

Figure 1.a): Schematic illustration of the proposed pipe strength estimation framework

(b) Status Update of Past Quarter Activities

<u>SECTION 1:</u>

<u>Task 1. Experimental testing and data analysis of chemical, metallurgical, and mechanical properties of pipe steel</u>

Summary

Several literature studies were carried out as a part of the previous quarters activities to understand the generic behaviour of the present system under study. This included studying the chemical and mechanical properties, such as composition, microstructure, stress-strain behaviour etc., for the different grades of linepipe steel and obtaining the statistical correlations were obtained between Yield strength and material properties. In the present quarter, this has been further extended to obtain the statistical correlations between Tensile Strength and the different material properties viz chemical and microstructural, to be used as likelihood functions in the Bayesian network fusion model.

And finally, methods for in-situ investigation of the toughness were in development, through the design of an ABI fixture.

Also, following on from the previous quarter activities, the different experiments conducted on the service linepipe steel samples obtained from GTI from one particular year of manufacturing, have been extended to another sample from a different year. The experimental testing consisted of metallographic inspection through Optical/SEM, image analysis through Image J software, composition analysis through EDS and Hardness tests with the Leeb Ball Hardness Tester. To add to these, tensile test of flat strip specimens was also conducted. The experiments were conducted for different thickness of the samples in order to capture the material property variation from the surface to the bulk, and an Ultrasonic thickness gauge was used to verify the thickness for the same. Another direction explored as a part of this study was to look into microstructure-property based model, in order to capture the mechanical property variation from surface to bulk with the help of a 3-D stochastic reconstruction model. And finally, the preliminary Bayesian Network model was further improvised to integrate the different components and provide a more accurate estimate of the probabilistic pipe strength and toughness.

Content

Samples from GTI:

The following service pipeline samples were obtained from GTI, as mentioned earlier, with the information of the installation year. The suspected grade and corresponding microstructures were obtained from the literature, based on the year of installation [1]. Two of these samples (pipe no. 45 & 47), marked with a highlighting have been used for the present study.

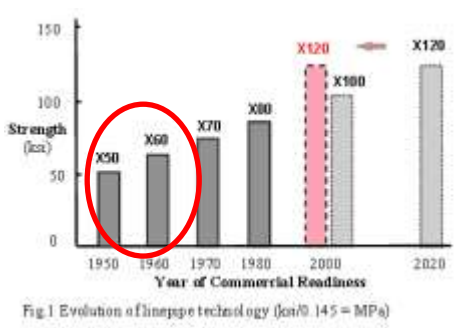

Figure 2: Development of pipeline steels [1]

Table1: Pipe samples and suspected grades

Pipe Number	Installation year	Pipe grade	Suspected grade	Suspected microstructures
24	2004	1522H	X100	BAINITE + MARTENSITE or bainite laths and M/A packets
32	1958	1522H	X60-X70	FERRITE PEARLITE
35	1961	1010	X60	FERRITE PEARLITE
44	Unknown	1513		Unknown
45	1949	1525	X50	FERRITE PEARLITE
47	1964	1025	X60	FERRITE PEARLITE

Experimental testing

1. Microstructure Examination:

In the previous report, the procedure for sample preparation to perform the metallographic inspection was included, along with measuring the thickness with the thickness gauge set-up was shown. The results for the two pipe specimens showed that as the sample is traversed along the thickness direction for pipe 45, the micrographs in the middle region depict a certain texture i.e. the phases are elongated along one direction (transverse). The samples from the second pipeline segment (pipe 47) did not a significant change in the microstructure while traversing through the thickness. As the manufacturing information isn't available, it is hard to say what may be the exact cause to generate such a trend.

The micrographs are presented below for the purpose of reference, until the middle region which is symmetric across the same by the inside and outside surfaces.

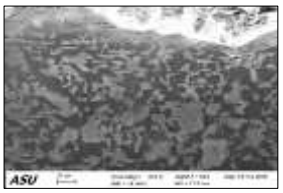

Fig:3. a) Edge 1

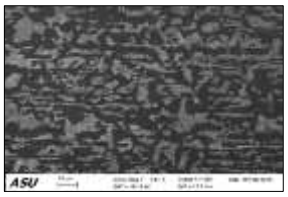

Fig.3: b) Edge 2

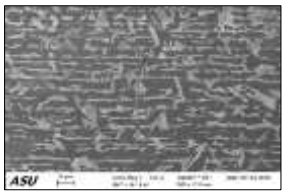

Fig.3 c) Edge 3

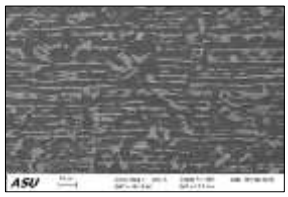

Fig.3: d) Edge 4

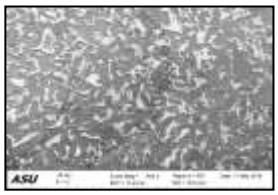

Fig.4: a) Edge 1

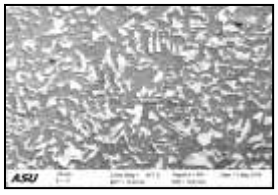

Fig.4: b) Edge 2

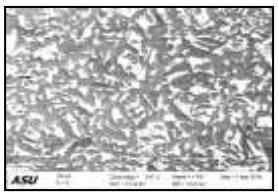

Fig.4: c) Edge 3

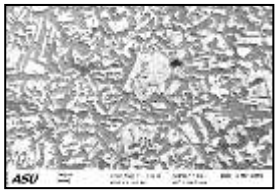

Fig.4: d) Edge 4

In the present work, the impact of the microstructure on the mechanical properties such as hardness, Yield strength and Tensile strength has been studied.

2. Tensile Test

In order to understand the impact of the microstructure on the mechanical properties, a tensile test was conducted on both samples, where the samples were extracted from the several layers along the pipe wall thickness. Tensile test procedure conformed to the requirements of API 5L [2]. Flat strip tensile test specimens were carved out of the pipe specimens for this purpose.

The procedure to obtain the samples was explained in the previous report which constituted the part with Pipe 45. It should be noted that flat strip samples were extracted from the entire thickness range of the pipe specimen to accurately capture material properties variation in the z-direction. With the given total thickness of the sample being about 8 mm, four flat strip tensile specimens of 1 mm thickness were extracted out from inner diameter portion to the outer diameter edge for both the pipes.

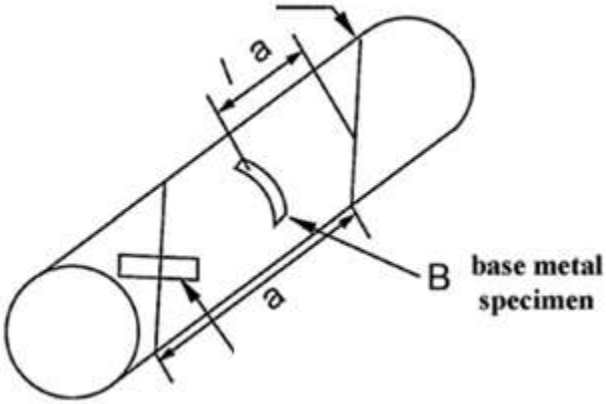

Figure 5a: Orientation of flat strip tensile specimen within the pipe sample [8].

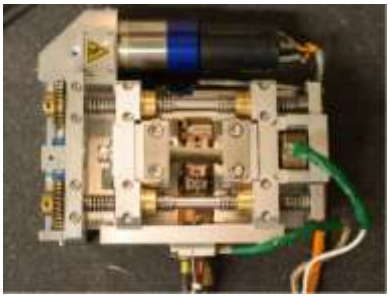

Figure 5b: Dimension of flat strip tensile specimens

The test equipment employed for this purpose was a small scale tensile stage machine, to be able to successfully support the flat strip samples and measure the mechanical properties. All tensile experiments were conducted at room temperature under displacement control with a strain rate of 0.05 mm/s. In each test, the applied load and specimen elongation were measured. Results were obtained in terms of yield strength (at 0.5% total elongation according to API 5L), ultimate tensile strength (UTS), and specimen elongation (in 50 mm gauge length) at fracture point for each test.

The dimensions for the two specimens are shown as below:

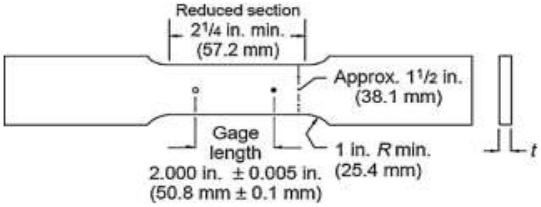

Pipe 45

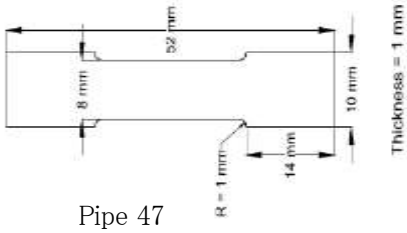

Pipe 47

Figure 6: Dimensions of flat strip tensile specimens

The dimensions of Pipe 47 were modified to have a custom design suited for the tensile stage machine to be able to reach the breakage point

The following table and chart lists the results obtained from the four samples:

Pipe 45:

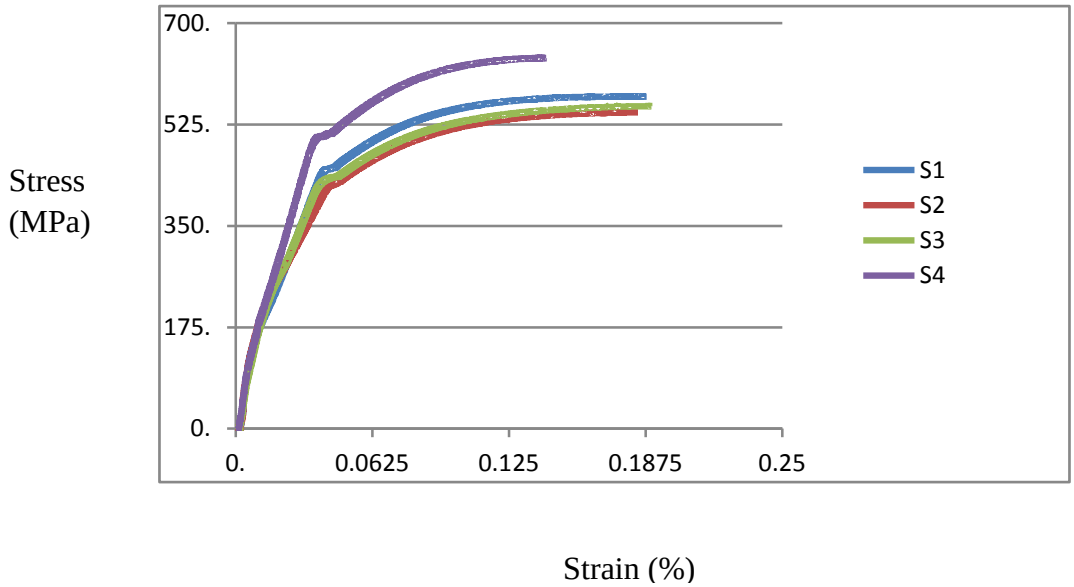

Figure 7a: Stress-Strain plot for the tensile test data

Table 2: YS and UTS of the samples

Samples	YS (MPa)	UTS (MPa)
S1(Top Layer)	450	572.99
S2(Layer 2)	425	538.4
S3(Layer 3)	435	555.6
S4(Layer 4)	506	637.5

The samples were labeled from S1 to S4 starting from the top to the bottom edge through the thickness. It was observed that the samples from the inner and outer surfaces depict a Yield and Tensile strength higher as compared to the middle sections, which can be correlated to the microstructure patterns in the different regions, as the load applied was in a direction perpendicular to the phase elongation direction which would break them by shear resulting in lower strength in the middle sections.

Pipe 47:

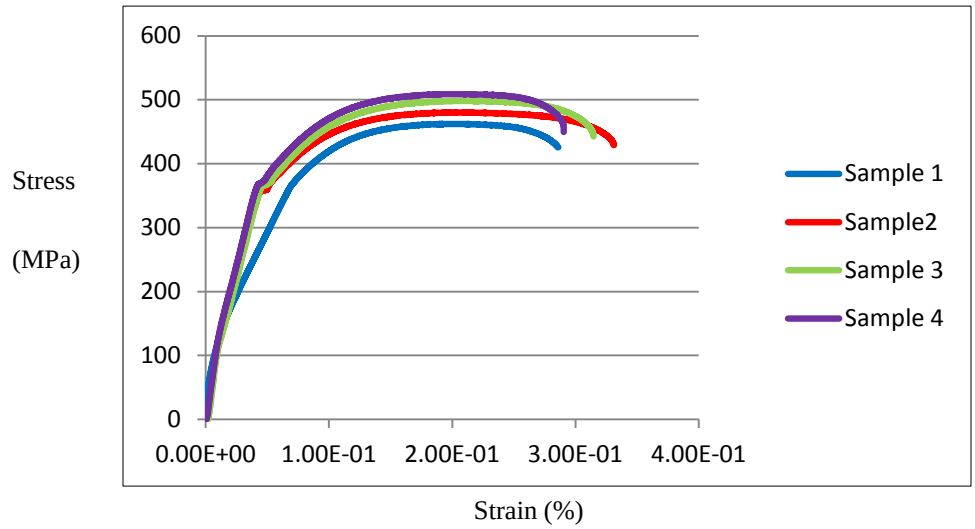

Figure 7b: Stress-Strain plot for the tensile test data

Table 3: YS and UTS of the samples

Samples	YS (MPa)	UTS (MPa)
S1(Top Layer)	355.5	462.2
S2(Layer 2)	358.4	479.4
S3(Layer 3)	366.2	497.8
S4(Layer 4)	371.08	508.4

This particular pipe 47 showed that the strength gradually increases upon moving from the outer surface to the inner edge. As this cannot be attributed to direct microstructure with phases, other material properties can be analyzed to investigate the trend in this behavior.

3. Hardness:

The **Vickers Hardness Tester** was used to examine the hardness of the samples, in order to determine the surface variation of hardness in the direction of the pipe wall thickness.

The following tables show the results for the same for the two pipe samples; Sample 1 represents the outermost surface exposed to the surrounding going towards the thickness being represented by samples 2 and 3, and sample 4 being the one towards the inner surface of the pipe.

Table 4a: Hardness of the pipe samples (HV); Pipe 45

Sample No.	Hardness (HV) H1	Hardness (HV) H2	Hardness (HV) H3	Mean Hardness (HV)
1	203.4	218.3	238.9	220.2
2	177	164.3	192.7	178
3	200.09	210.9	198.2	203.06
4	220.6	214.1	223.2	219.3

Table 4b: Hardness of the pipe samples (HV); Pipe 47

Sample No.	Hardness (HV) H1	Hardness (HV) H2	Hardness (HV) H3	Mean Hardness (HV)
1	212.6	211.5	200.4	208.17
2	214	216	221.8	217.27
3	207.2	217.7	240.3	221.73
4	225.5	211.4	241.2	226.03

The results have been plotted for the purpose of comparison;

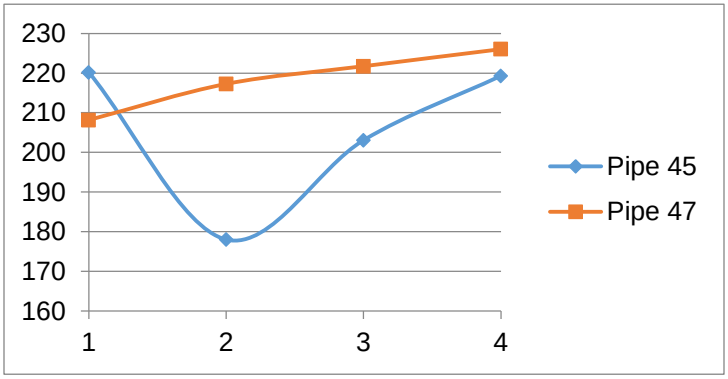

Figure 8: Hardness ;Pipe 45 vs 47

The hardness of the materials also was observed to be in line with the tensile properties; for Pipe 45, the middle regions had lower hardness and the edges or the surface regions had a higher value while the second pipe 47 showed a gradual increase in the hardness on progressing from the outer towards the inner diameter. This helps to further ascertain the behavior in the tensile properties and as such show the mechanical property variation along the pipe wall thickness. A material property investigation is made to investigate the cause of this behavior.

4. EDS Analysis:

In the previous quarter study, the chemical composition of the pipeline segment was obtained through semi-quantitative EDS with EPMA - JXA-8530F (JEOL) equipment using the point analysis method in the several regions and averaging the composition, as shown by the images below:

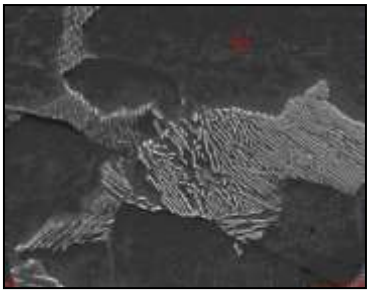

Figure 9a: SEM Image

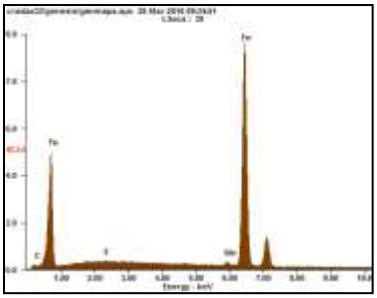

Figure 9b: EDS Spectrum

The beams were pointed at both the white and dark regions corresponding to Ferrite and Pearlite and the results were merged to obtain a quantitative weight percentage average.

Table 5a: Composition (Weight percentage)

Distance from the outer diameter edge (mm)	Elemental Composition (%)								
	Fe	C	N	Si	V	Cr	Mn	Ni	Mo
0.6	96.84	1.37	0.24	0.11	0.03	0.03	1.23	0.30	0.14
1	97.52	0.99	-	0.13	0.03	0.06	1.28	0.26	0.11
1.5	97.23	1.05	-	0.07	0.02	0.03	1.26	0.29	0.10
2	96.29	1.74	0.5	0.1	0.03	0.08	1.28	0.27	0.09
3	96.51	2.72	0.21	0.08	0.01	0.03	1.24	0.21	0.06
3.5	97.47	1.43	-	0.07	0.03	0.03	1.19	0.24	0.10
4	94.84	3.43	0.06	0.06	0.03	0.01	1.20	0.30	0.12
5	96.83	1.46	0.09	0.05	0.03	0.03	1.32	0.25	-
5.5	97.17	1.11	0.07	0.05	0.05	0.03	1.31	0.24	0.03

The elements of interest were chosen based on their direct or indirect correlation to the strength and fracture toughness, obtained from literature, governed by certain equations. The primary elements of interest were Fe, C, N, Si, V, Cr, Mn, Ni and Mo, however some of these were observed to be present only in trace amounts and were accounted for reference.

The purpose of the composition analysis for Pipe 47 at the present stage is to look for any compositional variation along the thickness of the wall and correlate the same with the mechanical property variation.

For Pipe 45, Small variation was shown by the trace elements along the thickness direction, and the maximum variation was observed by Carbon, however it did not show a trend corresponding to the microstructure. As the percentage of Carbon seemed to be way more than to be observed in a pipeline grade X50-X60, which could be due to the spot analysis, the next analysis for Pipe 47 were acquired using a phase map to obtain a direct average composition. In order to find out the cause of the mechanical property

variation, the composition was analyzed for Pipe 47, as microstructure did not show a considerable change. The phase maps of several elements are presented below:

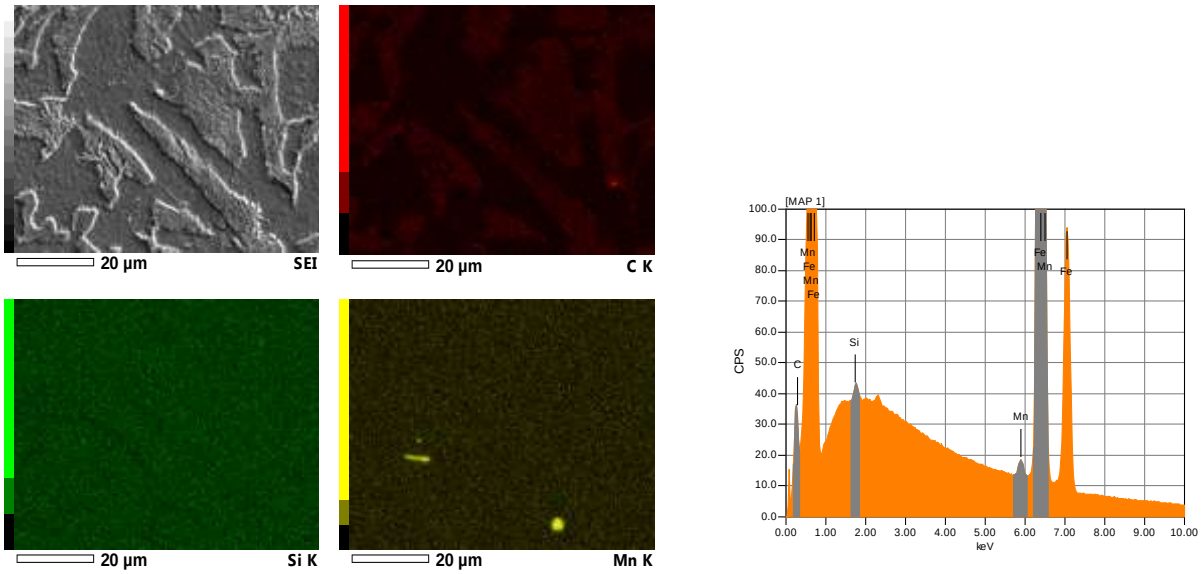

Figure 10: Phase maps of various elements

The above images depict the intensities of these elements in the different regions, and the corresponding one gets highlighted or brighter reflecting a greater intensity in that region. From the above picture, it can be observed that while most trace elements are just distributed evenly, C is the only one with higher concentrations pertaining to a certain region (pearlite), which is the case as pearlite is a carbon compound. The corresponding weight fractions are listed below, with a few trace elements and predominantly focusing on Carbon variation:

Table 5b: Composition (Weight percentage)

Distance from the outer diameter edge (mm)	Elemental Composition (%)			
	Fe	C	Mn	Si
1	98.39	0.82	0.73	0.05
2	98.10	1.11	0.76	0.04
3	98.21	0.91	0.85	0.04
4	97.97	1.13	0.86	0.04
5	97.99	1.05	0.90	0.06
6	98.46	0.79	0.05	0.70
7	98.38	0.83	0.05	0.73

.

The results of Pipe 47 again did not show a considerable trend in the variation across the thickness and hence cannot be attributed to being the direct cause of the mechanical property variation. Also, although C shows value in the 1 percent range, it is still too high for the grade of steel, and therefore, other techniques for composition analysis can be looked into, to confirm the compositon.

3D Stochastic Reconstruction:

In the previous work, the procedure to obtain a 3-D microstructure from a 2-D image was studied based on the stochastic reconstruction scheme developed by Yeong and Torquato [3]. This constituted of obtaining the key structural features, known as statistical descriptors are extracted from the 2D images that can contain various correlation functions (2-point correlation function in the present case), starting with a random state and calculating energy of the system, and continuing the same with performing random pixel change and accepting the energy change by Metropolis method [3], followed by the simulation annealing procedure to evolve the system to a state of global minimum energy.

In the present state, the reconstructions have been performed from the isotropic and the anisotropic portions of the images from Pipe 45, with results shown below:

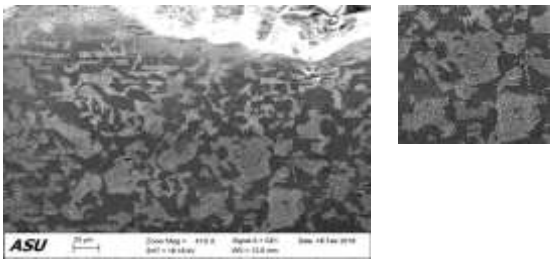

Fig.11 a): Raw Images

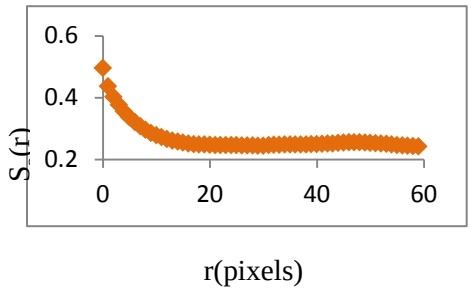

Fig.11 b): 2D Correlation function

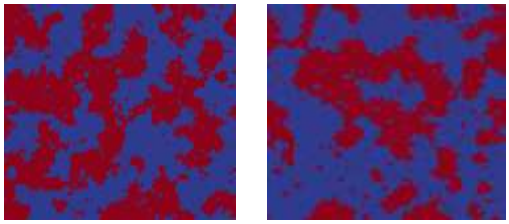

Fig.11 c): 2D slices

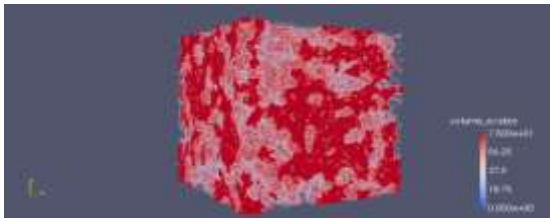

Fig.11 d): 3D Reconstruction

The isotropic portions above show a good relation for the 3-D reconstructed image. The anisotropic portions are shown below:

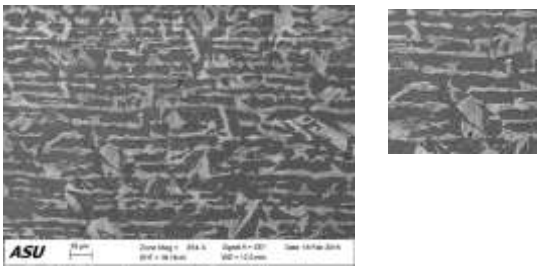

Fig.12 a): Raw Images

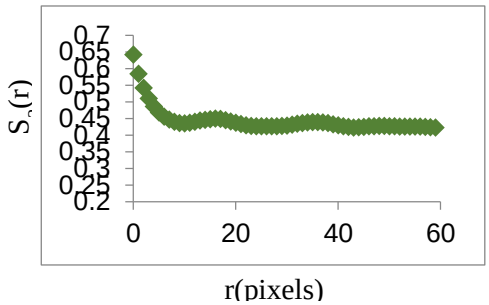

Fig.12 b): 2D Correlation

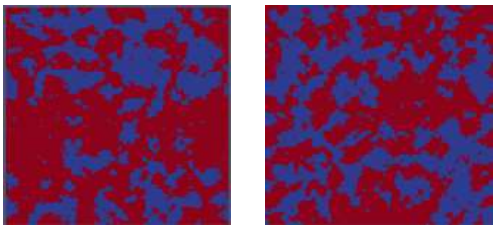

Fig.12 c): 2D slices

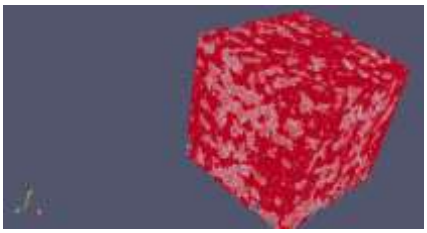

Fig.12 d): 3D Reconstruction

The anisotropic portion however, doesn't show a very good representation of the two dimensional image, and hence would be further analyzed in the future.

Task 3. Bayesian network for information fusion and probabilistic pipe strength estimation

The Bayesian Network model, developed with the use of an open source software WINBUGS, was tested for extraction of further features. This is based on the general Bayes theorem [4].

The following correlations between Yield Strength, Ultimate Tensile Strength and the different material properties have been utilized from the literature;

YS= 53.9 + 32.34(Mn) +83.2(Si) +354.2(N_f) + 17.4 (d -1/2) [5]
where Mn – Mn content (%), Si – Si content (%), N_f - free N content (%), and d -ferrite grain size (in mm)
YS(f/p)= YS(f) (V_f) + YS(p) (1-V_f) [6,7],
Where YS(f/p) is the yield strength of the dual phase material, YS(f) is the yield strength of the ferritic phase and YS(p) is the yield strength of the pearlite phase. Vf is the volume fraction of ferrite.
YS=2* H+105 [8], where H - Vickers hardness
Also, TS = 1.3 × H + 344 [8], where H-Hardness
TS = 294.1 + 27.7(Mn) + 83.2(Si) + 3.9(P) + 7.7(d-2) [5], where P is the pearlite content in the matrix and the other symbols have the usual meanings.

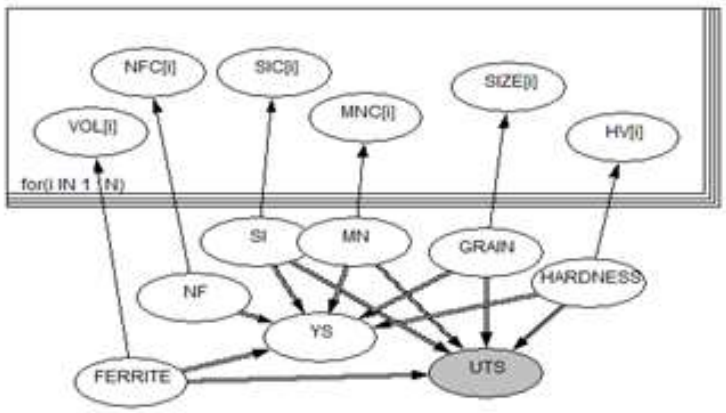

Figure.13: BN Model for YS and UTS determination

Features:

1. Reduced Uncertainty and Convergence:

The box loop is capable of handling multiple data sets and uses one data set at a time and estimates a posterior distribution which forms a prior for the subsequent analysis. The large amount of data helps reduce the variability whereas the latter helps the system to converge.

2. Node Sensitivity:

The model is capable of predicting the dependency of one node on another, in a quantitative manner. This was validated by assigning same weightage to all the statistical correlations and testing for the value of Yield strength to be comparable with the theoretical one, which turned out to be more sensitive to the Hardness, grain size and composition, but less to the phase volume fraction, and hence more time can be devoted to the study of the high impact parameters.

3. Capability to update the other nodes:

All the nodes in the system can be updated, irrespective of a direct or indirect correlation with the updating node. This helps to converge the parameter values and quantifying the uncertainty of the system as the model is updated in the view of new information from various measurements [9].

a) Addition of the node UTS followed by change in YS and Hardness:

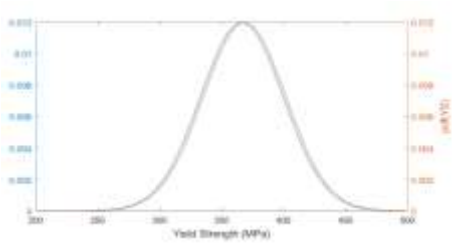

Fig.14 a)

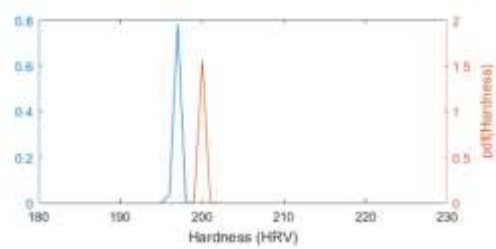

Fig.14 b)

b) With or without being provided with a measurement node for hardness (HV); change in node SI:

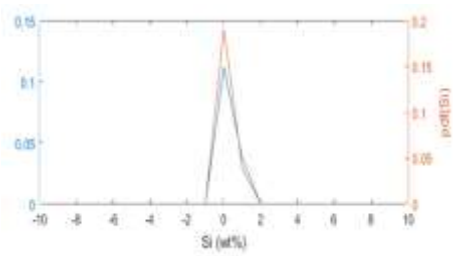

Fig.14 c)

References:

1. J.Y.Koo,M.J.Luton,M.V.Bangan,R.A.Petkovi. Metallurgical Design of ultra-Strength steel for Gas pipeline.

2. API Specifications 5L, Specifications for line pipe, forty-third ed., American Petroleum Institute, 2004.

3. C. L. Y. Yeong and S. Torquato, Phys. Rev. E 57, 495 (1998).

4. Liu, W., K. Yue, and J. Zhang, Augmenting learning function to Bayesian network inferences with maximum likelihood parameters. Expert Systems with Applications, 2009. **36**(2, Part 2): p. 3497-3504

5. Bruce L. Bramfitt (1998). Structure/Property Relationships in Irons and Steel, *Bethlehem Steel Corporation. ASM International.*

6. Thomas Hoper.Shigeru Endo.Nobuyuki Ihikawa and Koichi Osawa (1999). Effect of Volume Fraction of Constituent phases on the stress-strain relationship of Dual Phase Steels. *ISIJ International, Vol. 39.*

7. Zhonghua Li a, S. Schmauder b, M. Dong b. A simple mechanical model to predict fracture and yield strengths of particulate two-phase materials. *Computational Materials Science 15 (1999) 11-21*

8. S.H. Hashemi (2010). Strength–hardness statistical correlation in API X65 steel, *Materials Science and Engineering A 528 (2011) 1648–1655*

9. Ma, Y., Wang, L., Zhang, J., Xiang, Y., Peng, T., and Liu, Y. (2014). "Hybrid Uncertainty Quantification for Probabilistic Corrosion Damage Prediction for Aging RC Bridges." *J. Mater. Civ. Eng., 10.1061/(ASCE)MT.1943-5533.0001096, 04014152.*

Planned activities for the next quarter:

- Grain Size analysis to investigate a trend in mechanical behavior of Pipe 47
- EDS/EBSD studies to obtain phase maps, compositions etc.
- Microstructure, composition analysis for tensile specimens to validate the functional correlations in the present BN model
- ABI test fixture design to extract other mechanical properties; Fracture Toughness
- Update the preliminary BN model to predict Fracture Toughness
- Data training of the model to integrate the surface and bulk measurements
- Replicating the BN Model in Matlab; data handling & continuous likelihood functions
- 3-D stochastic reconstruction for the anisotropic sections and other specimens.

Automated Ball Indentation Test fixture design

As the conventional mechanical tests require large test specimens, which may not be feasible for pipes in service. Therefore, it is of great importance to develop methods which can be performed in-situ. Since the testing is carried out in-situ, it needs to be non-destructive or minimally destructive in order to serve the purpose of testing [1]. The automated ball indentation (ABI) test is based on strain-controlled multiple indentations (at the same penetration location) of a polished surface by a spherical indenter (0.25 to 1.57-mm diameter). The microprobe system and test methods are based on well demonstrated and accepted physical and mathematical relationships which govern metal behaviour under multiaxial indentation loading [2]. The objective of the research project

is to predict the through thickness mechanical properties (toughness, yield strength, ultimate tensile strength etc.) of a material specimen using ABI testing.

1. Previous Work:

An electromechanical MTS testing machine, capable of a maximum loading of 10kN is used to carry out the ABI testing. Fixtures to hold the indenter and specimen were designed for the machine. The displacement and load of the indenter can be monitored via Testworks software by MTS. A MATLAB code to obtain the stress-strain curve from experimental data has been written. The stress-strain was obtained by solving non-linear equations iteratively. In order to validate the code, the stress-strain curve is compared with literature data for stainless steel by Fahmy Haggag et. al [4]. A finite element model to simulate the testing has been generated with a single loading case for the indentation in the plate specimen. Thereafter, the finite element model was extended to include multiple loading and unloading cases similar to a real ABI test. The stress-strain data to feed in the Abaqus model is taken from the results obtained from the code in MATLAB developed previously.

2. Finite Element Model:

The indenter is considered to be an analytical rigid body, given its high hardness and the plate material is considered to be steel with elastic-plastic deformation occurring due to the contact. The material properties used for the steel plate are summarized as given below:

Modulus of Elasticity – 210.7GPa

Poisson's Ratio – 0.303

Yield stress (MPa)	Plastic Strain
331.0	0
452.2029	0.0315
583.4558	0.0451
617.5216	0.0579
651.6218	0.0833
704.1682	0.1012
722.5844	0.1176
747.9392	0.1305
763.1123	0.1418
787.0135	0.1511

Table 1. Plastic properties for steel

Boundary conditions are applied on the plate and indenter so as to simulate the contact of the pair. The bottom face of the plate was fixed and the load is applied on the top face of the indenter. While defining the contact pair, the plate is made the master surface whereas the indenter is considered as the slave surface. The thickness of the plate specimen was considered to be 12mm for the results. Figure 1 shows the comparison of the load – displacement curve of the actual testing data from literature [1] and the results from the simulation in Abaqus. It can be seen from the figure that the loading force in the simulation is higher as compared to the real testing data. The reasons for the difference between the real testing data and simulation can be given as follows:

1. The indenter is modelled as analytical rigid, creating a stiffer response
2. The material properties (stress-strain curve) of the steel specimen model
3. The thickness of the plate specimen considered for the simulation

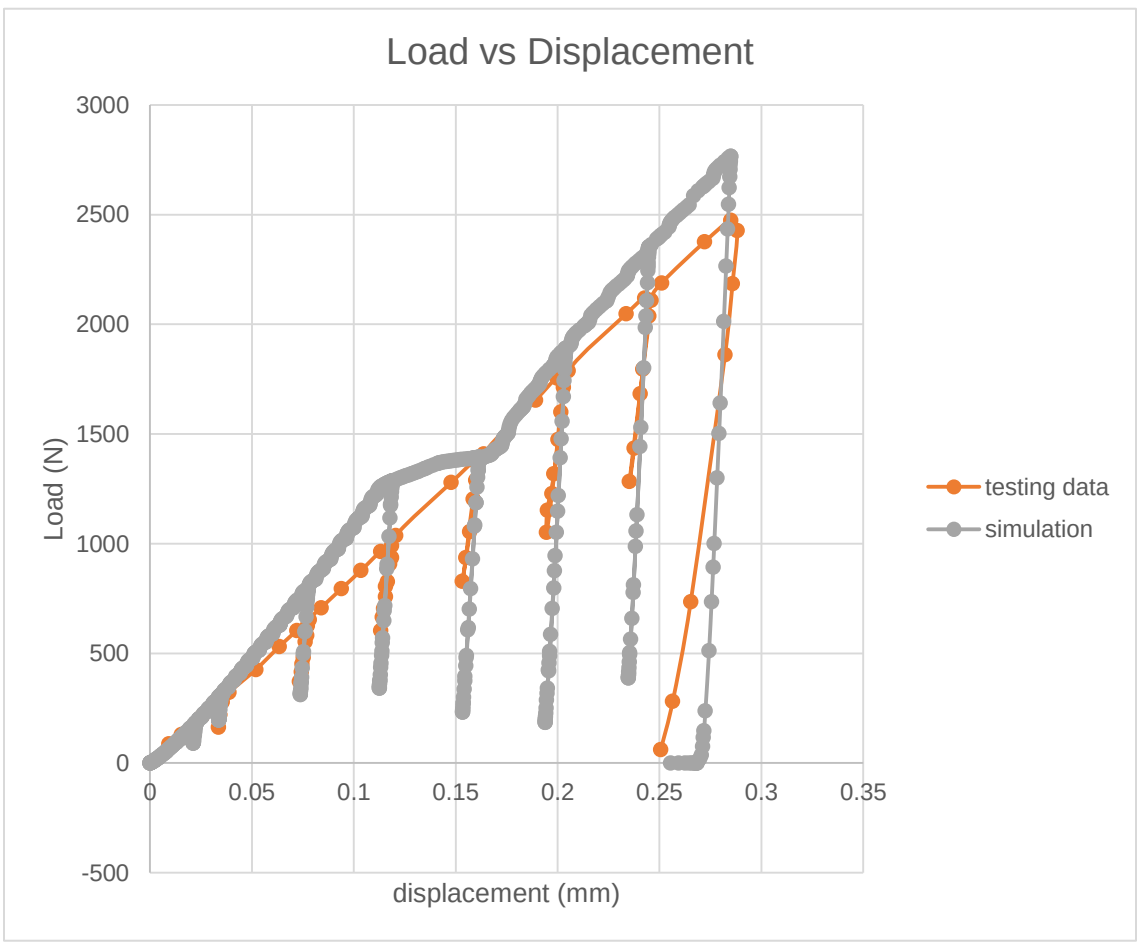

Figure 1 plot of load-displacement from the simulation and the literature

The model was meshed using various control parameters such as edge divisions to achieve good quality elements in the desired region. A displacement controlled loading-unloading curve with 8 cycles is simulated for displacement controlled model from literature [4]. From, the simulation, it can be seen that the plate relaxes slightly in

the unloading cycles, retaining the plastic strain in the plate specimen.

3. Future Scope:

- Conduct a study by simulating the through thickness properties of pipe specimens.
- Create a response surface by performing a design of experiments on the surface properties to predict the through thickness properties

References:

1. Das, M., Pal, T. K., and Das, G., 2012, "Use of Portable Automated Ball Indentation System to Evaluate Mechanical Properties of Steel Pipes," Trans. Indian Inst. Met., **65**(2), pp. 197–203.
2. Haggag, F. M., 1993, "In-situ measurements of mechanical properties using novel automated ball indentation system," ASTM Spec. Tech. Publ., pp. 27–44.

SECTION 2:

Task 2.1 PA simulation and experiment validation

Several finite element models have been simulated by using ANSYS. The purpose of these models is to present and improve the numerical model to predict the mechanical behavior and electromagnetic behavior under displacement and validate with the experiment result. As shown in the figure 1, the 3D solid element 185 is used for the analysis.

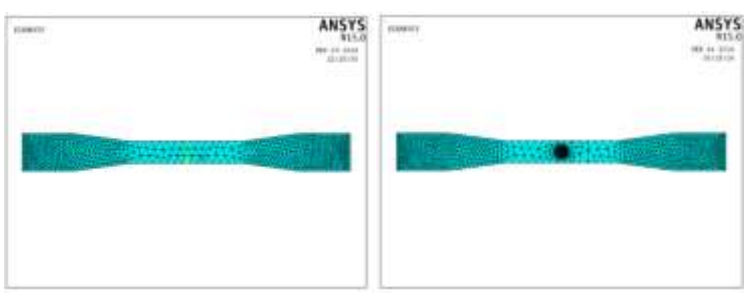

Figure.1 mechanical model of the specimens

The left boundary of specimens where X = -82.5 is limited as fixed support in all directions and restrict the rotation and translation. The load simulation is same as the experiment; the displacement is applied to the right end of the specimen where x = 82.5mm along the x direction. For both specimens they have been simulated and elongated at different percentages as shown in the following table.

Specimen type	Max. Elongation (mm)	30% elongation (mm)	50% elongation (mm)	70% elongation(mm)
full specimen	129.1082	38.735	64.5414	90.3732
notched specimen	33.02	9.906	16.51	23.114

Table .1 Specimens elongation [1]

The electromagnetic field simulation is implemented after the mechanical simulation. As figure shown below, the result of the mechanical simulation is used as the input of e-field simulation.

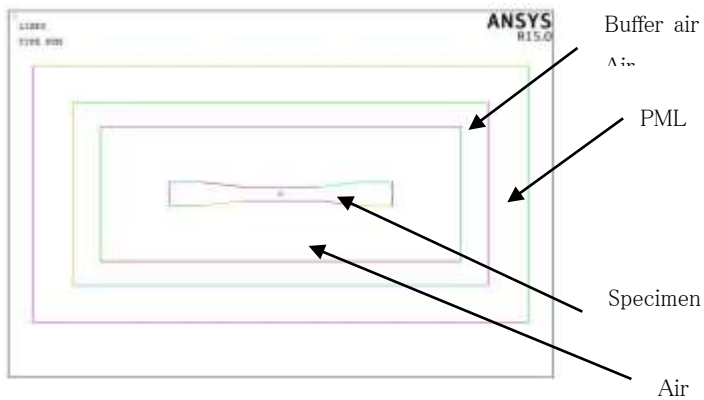

Figure.2 electromagnetic model

The outermost layer is the perfectly matched layer with thickness 90mm and the second layer is the buffer air layer with thickness 60mm. Since PML acts as an infinite open domain, any boundary conditions and material properties need to be carried over into the PML region. It can reduce the size of the computational domain significantly with very small numerical reflections. We select section line along the hold root. The experiment result has been processed and smoothed with a shifting window.

$$E_i = \frac{\sum_{k=i}^{i+200} Scanningdata[k]}{200}$$

The 1-D plots of the E-field combine with the experiment result have been shown below.

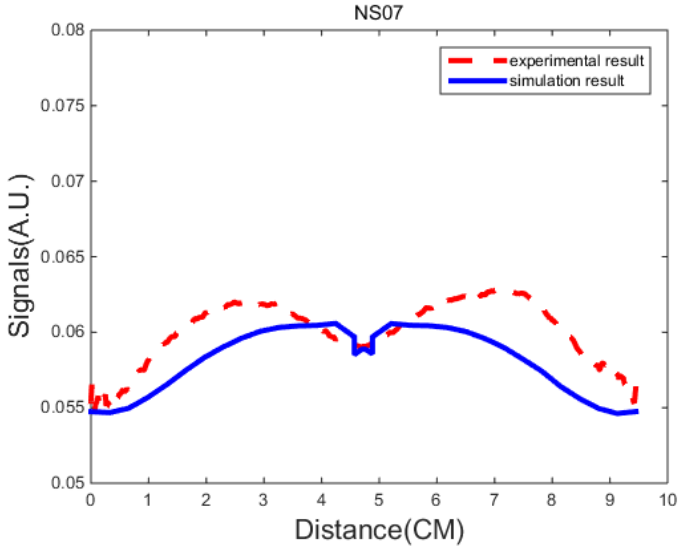

Figure.3 simulation and experiment result

As we can see in the image, the simulation result shows same trends as the experiment result except more sharp around the hole and the results are matching quite good.

Task 2.2 Steel specimens' simulation

The steel is the most widely used industrial material. The reason of steels' overwhelming dominance is the great variety of microstructures and achieve a very large range of desirable properties. Different internal microstructure of steel can be generated by solid-state transformation and processing [2]. Through changing the microstructure, we can obtain materials with different mechanical, physical and chemical properties. Take steel as an example, the strength and toughness can be decrease of several times. In Fe-C alloy there are several kinds of microstructures such as austenite, pearlite, martensite, and bainite, the different microstructure has produced the corresponding material property.
Austenite is solid solution formed in the iron with face-centered cubic structures. It has high plasticity and low yield strength and Stable in the high temperature region.
Therefore, the plastic deformation processing of the steel is usually presence of the high temperature. Pearlite is composed of eutectoid ferrite and cementite. Lamellar spacing of lamellar pearlite has certain influence on strength and plasticity, the smaller pearlite lamellar spacing is, the higher strength and plasticity would achieve.
Martensite is the crystal structure of body centered cubic or body-centered tetragonal. The main features of martensite are high hardness and high strength [2] [3].
Since the microstructure has a great influence on the performance of the materials, it is very important to have an accurate and reliable measurement. Several multi physics simulations of the steel (Q235) under different displacements have been simulated. The models have been simulated both around and lower the material yield strength. When the

stress exceeds the yield point, the transformations of the microstructure will result in the changing of the steel's elastic modulus.

	1st simulation	2nd simulation	3rd simulation
Displacement(mm)	0.181	0.1295	0.096

Table.2 displacements of the simulation

The nephograms and the plots have been shown in the following figures.

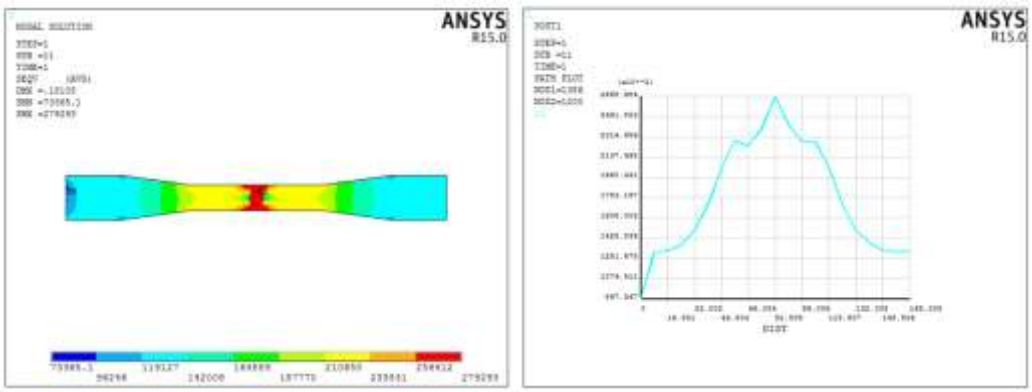

Von Mises stress

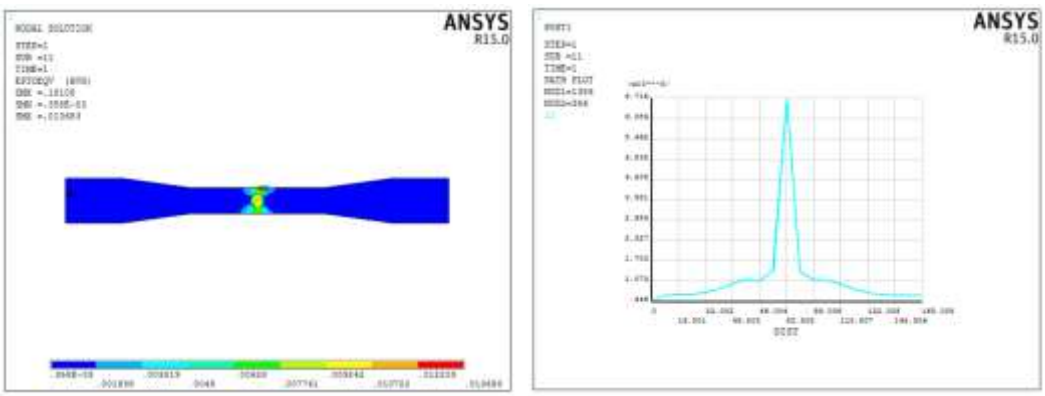

Von Mises strain

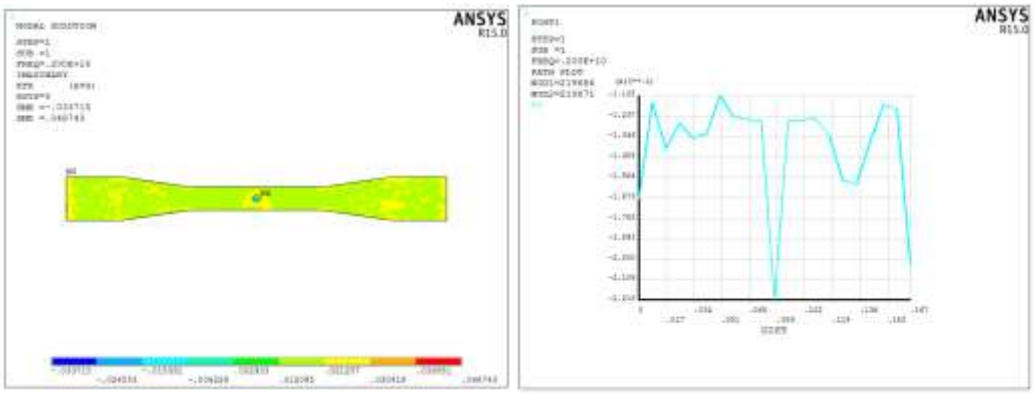

E-field on the surface

Figure.4 the specimen with 0.181mm displacement

For the E-field in the first simulation, the line reaches the bottom at the center where the hole is located. The E-field remains the same value for a short distance beside the hole and the strain plot shows the same trend at corresponding location.

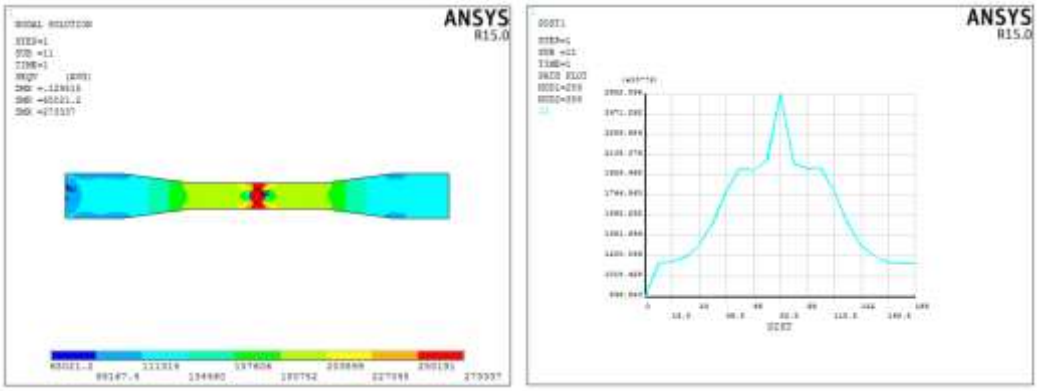

Von Mises stress

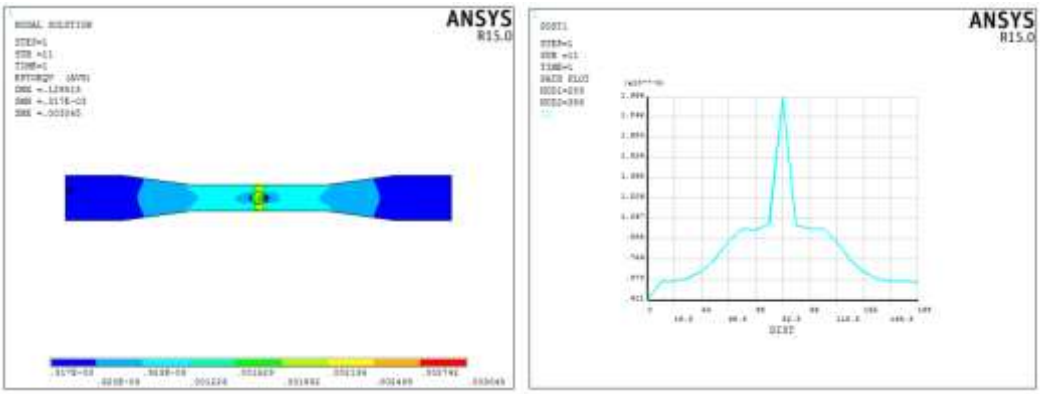

Von Mises strain

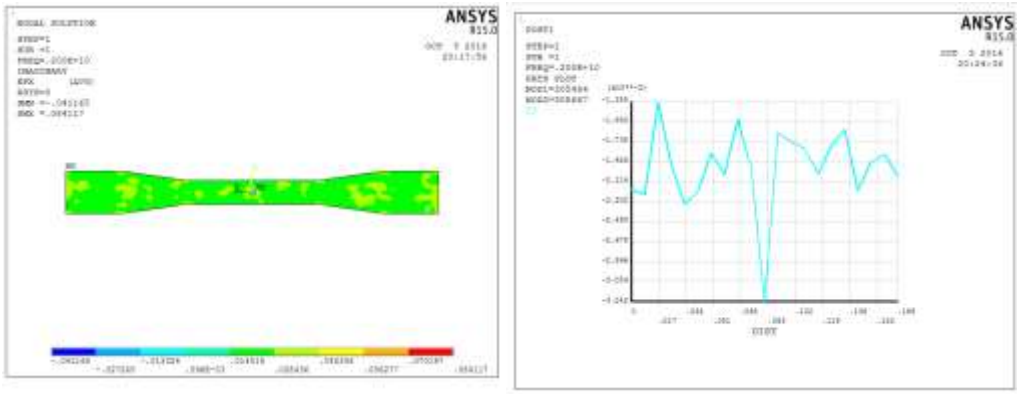

E-field on the surface

Figure.5 the specimen with 0.1295mm displacement

Since the displacement of the second simulation is less than the first one, the maximum strain is reduced and the slope of the line near the center is smaller. The plot of the E-field experience larger oscillation beside the hole.

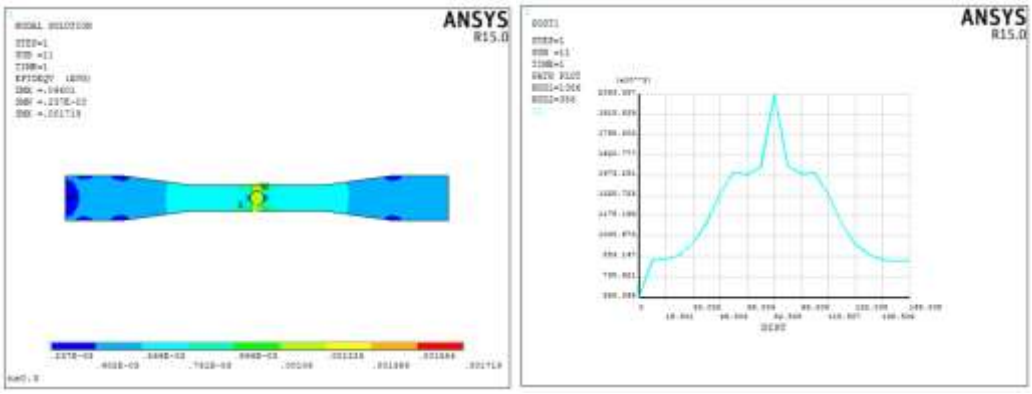

Von Mises stress

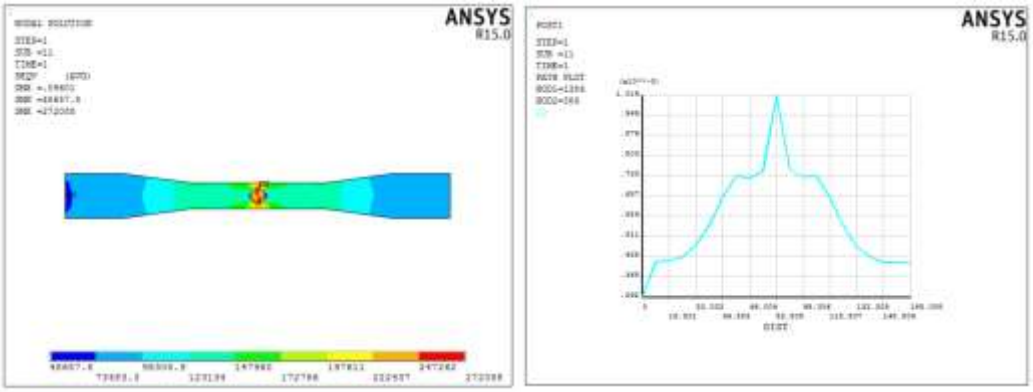

Von Mises strain

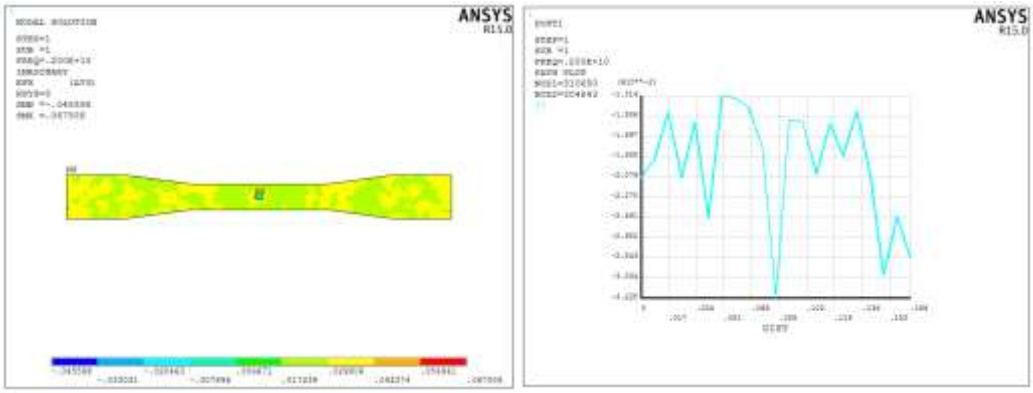

E-field on the surface

Figure.6 the specimen with 0.096mm displacement

As shown in the above figures, the stress and strain of the specimens is symmetrical. Due to the hole in the center of the test piece, the maximum stress is generated when the displacement is applied to the hole position. The stress and strain gradually decreases on both sides of the symmetrically. With the increase of external deformation, the tissue will contain more and more deformed crystals. According to the stress and strain nephograms, the number of microstructure changed in the specimens is also the largest in the middle

and are symmetrically reduced to each end. In structural analysis, the displacement of the structure will result in the structure deformation. It not only changes the shape and size of the specimen, but also will also transform the internal organization and related performance. As the displacement increased, the E-field shows less oscillation. In the simulation with the largest displacement, the E-field shows the trends as a platform beside the hole while the strain experience the same trends. More simulation will be done by ANSYS and ABAQUS to study the relation between the mechanical properties and micro-electromagnetic properties.

Task 2.3 Post processing of scanning result

The scanning images of near-field microwave microscopy are blurred in the axial direction by contributions of point spread function and also contain noise. Therefore, the Post processing of scanning result is very necessary to improve the image. Image segmentation is a technique that split and subdivide a digital image into several segments which able to simplify the image, extract the information and make the image easier to analyze [4]. A better performance of de-noise and deconvolution can be achieved with the good segmentation. The edge can be detected and extracted from the image by find the pixels with similar computed property. Although segmentation can use the higher order derivatives in principle, first order and second order derivative is most commonly used since higher order derivatives might sensitivity to the noise. The second order derivative can explain the change of the gray intensity. The magnitude and direction of the gradient are calculated using the first order partial differential by using follow equation

$$f_x'(x,y) \approx G_x = \frac{[f(x+1,y) - f(x,y) + f(x+1,y+1) - f(x,y+1)]}{2}$$
$$f_y'(x,y) \approx G_y = \frac{[f(x+1,y) - f(x,y) + f(x+1,y+1) - f(x,y+1)]}{2}$$

Where G_x and G_y is showing at follow:

G_x		G_y	
1	-1	-1	-1
1	-1	1	1

Solve the partial differential equation within this 2 by 2 square to get the magnitude and direction.

$$\mathrm{M[x,y]} = \sqrt{G_x(x,y)^2 + G_y(x,y)^2}$$

$$\theta[x, y] = \arctan\left(\frac{G_x(x, y)}{G_y(x, y)}\right)$$

By non-maxima suppression and connecting the edges, the edge information can be extracted from the image.

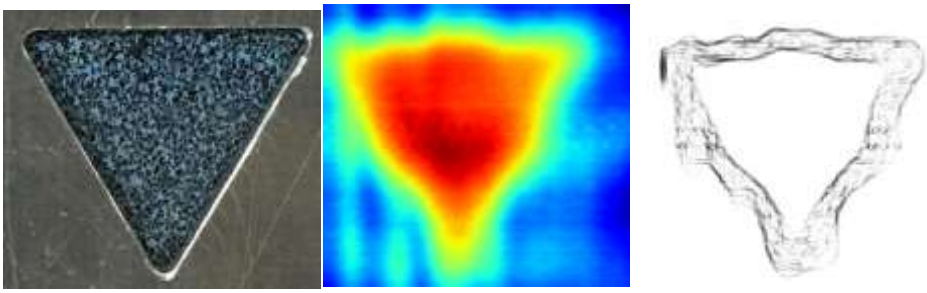

Figure.7 segmentation of the triangle

The figure shown above is the scanning result of a steel with a triangle hole in the middle and the result of the segmentation.

Reference:

[1] Desai, K.S & Kardile, K(2016). Optimized Diagnosis and Prognosis for Impingement Failure of PA and PE Piping Materials [slides]

[2] Bhadeshia, H. K. D. H, & Honeycombe, R. W. K. (2006;2011;). Steels: Microstructure and properties (3rd;3; ed.). Amsterdam;Boston;: Elsevier, Butterworth-Heinemann.

[3] Dobmann,G. Physical Basics and Industrial Applications of 3MA – Micromagnetic Multiparameter Microstructure and Stress Analysis. Fraunhofer IZFP, Germany

[4] Pinoli, J., & Ebooks Corporation. (2014). Mathematical foundations of image processing and analysis. Hoboken, NJ;London;: ISTE.